The Journal of Chemical Physics

Describing adsorption of benzene, thiophene, and xenon on coinage metals by using the Zaremba–Kohn theory-based model

Cite as: J. Chem. Phys. **154**, 124705 (2021); https://doi.org/10.1063/5.0042719
Submitted: 03 January 2021 . Accepted: 07 March 2021 . Published Online: 23 March 2021

Santosh Adhikari, Niraj K. Nepal, Hong Tang, and Adrienn Ruzsinszky

The Journal of Chemical Physics ARTICLE scitation.org/journal/jcp

Describing adsorption of benzene, thiophene, and xenon on coinage metals by using the Zaremba–Kohn theory-based model

Cite as: J. Chem. Phys. 154, 124705 (2021); doi: 10.1063/5.0042719
Submitted: 3 January 2021 • Accepted: 7 March 2021 •
Published Online: 23 March 2021

Santosh Adhikari,[a] Niraj K. Nepal, Hong Tang, and Adrienn Ruzsinszky

AFFILIATIONS

Department of Physics, Temple University, Philadelphia, Pennsylvania 19122, USA

[a]Author to whom correspondence should be addressed: tuf60388@temple.edu

ABSTRACT

Semilocal (SL) density functional approximations (DFAs) are widely applied but have limitations due to their inability to incorporate long-range van der Waals (vdW) interaction. Non-local functionals (vdW-DF, VV10, and rVV10) or empirical methods (DFT+D, DFT+vdW, and DFT+MBD) are used with SL-DFAs to account for such missing interaction. The physisorption of a molecule on the surface of the coinage metals (Cu, Ag, and Au) is a typical example of systems where vdW interaction is significant. However, it is difficult to find a general method that reasonably describes both adsorption energy and geometry of even the simple prototypes of cyclic and heterocyclic aromatic molecules such as benzene (C_6H_6) and thiophene (C_4H_4S), respectively, with reasonable accuracy. In this work, we present an alternative scheme based on Zaremba–Kohn theory, called DFT+vdW-dZK. We show that unlike other popular methods, DFT+vdW-dZK and particularly SCAN+vdW-dZK give an accurate description of the physisorption of a rare-gas atom (xenon) and two small albeit diverse prototype organic molecules on the (111) surfaces of the coinage metals.

I. INTRODUCTION

The interface between the molecule and the surface involves the interplay of covalent and weak binding (dominated by vdW interaction), often guided by the nature of the molecule and surface. The choice of a particular molecule–surface system is driven by its possible applicability. While studies focus on graphene for designing sensors,[1,2] basal planes and more reactive edges of MoS_2 are recommended for heterogeneous catalysis.[3,4] Recently, the interface of an organic molecule and metallic surface has received much attention due to its wide application in diverse fields, such as optoelectronics, catalysis, sensors, and surface-photochemistry.[5–9] There are experimental techniques such as temperature-programmed desorption (TPD), normal-incidence X-ray standing wavefield absorption (NIXSW), and near-edge X-ray absorption fine structure spectroscopy (NEXAFS) to help determine the adsorption energy and geometry at the interface. However, experimental results are affected by surface defects, monolayer formation, the orientation of the adsorbate, etc., and require analysis from several experiments to be put together for the full picture.[7] These difficulties motivate the need for computational tools that are able to mimic the mechanism that requires a delicate balance between the short- and long-range interactions [mainly van der Waals (vdW) effect].[10–13] Being a nonlocal effect, the latter poses a tough challenge for theoretical methods.

Wave-function based approximations such as coupled-cluster (CC) can account for the vdW effect with greater accuracy but are computationally out of reach for such interface models. Alternatively, density functional theory (DFT)[14,15] provides a framework for electronic structure calculations in diverse fields[16] through different rungs of approximations illustrated by the Jacobs ladder of Perdew.[17] High-level approximations such as the random phase approximations (RPAs) within this framework are nearly exact for the long-range vdW effect.[18] However, despite the increased computational power and efficient implementation,[19] RPA is unable to handle supercell calculations involving a relatively large numbers of atoms. DFT can accommodate these calculations at the semilocal (SL) level, but the required long-range correlation effects are missing here. Therefore, SL density functional approximations (DFAs) are often combined with a nonlocal correlation functional[20–23] or an empirical method[24–33] that relies on input polarizabilities, mostly

through some adjustable parameters to include the vdW effects. These adjustable parameters guide the delicate balance between the short-range interactions captured by DFAs (base functionals) and the long-range interactions that the correction methods provide.[34]

GGAs (generalized gradient approximations) are superior to local-density approximation (LDA) for aromatic systems[35] and hence are the natural choices as base functionals. PBE[36] and its revised versions[37–39] and the Becke functionals[40–42] are some successful[43–50] base functionals at the GGA level. Despite being widely used, GGAs by themselves are unable to capture vdW interaction beyond the short-range, while the SCAN[51] metaGGA does. SCAN, by construction, can recognize different bonding environments. There are a few instances such as formation energies of weakly bound intermetallics[52–54] and prediction of magnetic properties of transition metals,[55] where SCAN is not up to the mark, but it has been mostly successful for diversely bonded systems.[56–60] Recently, SCAN was revised (revSCAN[61]) by diminishing its intermediate-ranged vdW interaction, leading to better interaction energies of molecules of the S22 dataset when combined with VV10[22] than SCAN+VV10. However, when combined with rVV10,[23] SCAN is remarkably accurate for molecular complexes, solids, and layered materials.[62]

Both VV10 and rVV10 are nonlocal correlation functionals like vdW-DFs,[20,21] paired with the base functional as

$$E_{xc} = E_{xc}^{DFA} + E_c^{nl}, \tag{1}$$

where E_{xc}^{DFA} is the total exchange–correlation energy computed from the base functional, while E_c^{nl} is the nonlocal electron-correlation energy. These schemes bridge the nonlocal correlation functionals to the semilocal functional through a few parameters and depend only on the electron density as input.

There is an alternative way to include the vdW interaction through empirical methods where the base functional is often combined as

$$E_{tot} = E_{DFA} + E_{vdW}, \tag{2}$$

where E_{DFA} is the total energy computed from the base functional, while E_{vdW} is the contribution to the total energy due to vdW interaction. Methods such as DFT+D[27,28] model the latter part as aC_6 coefficient-based pairwise additive interaction. The C_6 coefficients utilized here are unable to adjust to the chemical environment (system) and neglect the many-body dispersion effects. However, methods such as DFT+D3,[29,30] XDM[24–26] (exchange–hole dipole moment), and DFT+vdW[31] incorporate the information of the system through different ways.[34]

In our present assessment, we investigate the adsorption of benzene, thiophene, and xenon over the (111) surfaces of the coinage metals. Since the (111) surface is highly stable and cost-efficient, it is extensively used in catalysis.[63] Benzene (C_6H_6) and thiophene (C_4H_4S) are, respectively, the most studied[64–66] prototypes of the cyclic and the heterocyclic aromatic molecules. Benzene is the building block of an entire class of aromatic compounds having wide industrial applications. Through catalytic hydrogenation and oxidation, benzene can form various useful aromatic molecules such as phenol and nitrobenzene.[67–69] A recent theoretical study of adsorption of benzene, toluene, phenol, and m-cresol on transition metal surfaces reveals a weaker role of the functional group in adsorption compared to the phenyl ring itself.[70] This further justifies the choice of benzene as a test molecule. Similarly, thiophene is the smallest sulfur-containing polar aromatic compound found in petroleum products. An accurate description of the adsorption of thiophene is crucial for modeling hydrodesulfurization reactions.[71] Previous studies suggest organic molecules adsorbing strongly on both ferromagnetic metal surfaces (Fe and Ni) and platinum-group metal surfaces (Pt, Pd, and Rh).[35] As coinage metals have relatively inert d-bands, their reactivity lies between that of platinum-group metals and simple sp-metals such as Al.[35] Several past studies have suggested the physisorption of benzene, thiophene, and xenon on the coinage metal surfaces. The physisorption process is dominated by vdW interaction, making the organic-coinage metal interfaces ideal systems for assessing the vdW-corrected methods. Besides, benzene, thiophene, and xenon over coinage metals are well understood theoretically and experimentally.[31,33,44,45] The latter serves as a benchmark to evaluate the performance of the theoretical models.

Here, we evaluate the adsorption energies and distances of benzene, thiophene, and xenon over the (111) surfaces of the coinage metals using the recently proposed model[72] based on Zaremba–Kohn's second-order perturbation theory designed for modeling the physisorption of a particle over the surface. This model naturally incorporates the screening effects, which are missing in most empirical methods. It yields RPA quality results for the physisorption of graphene over metallic surfaces[72,73] and semiconducting layered materials.[74] It was also shown that when combined with PBE, this method outperforms all other semilocal functionals paired with rVV10 for the adsorption of thiophene on coinage metal surfaces (see details in Ref. 50). We note that the model DFT+vdW[32] is also based on Lifshitz–Zaremba–Kohn theory. However, that model includes the screening effects through the C_6 instead of C_3 coefficients and has no higher-order terms, such as quadrupolar C_5.

II. COMPUTATIONAL DETAILS

All the DFT calculations performed utilized the projector augmented wave (PAW) formalism as implemented in the Vienna *ab initio* simulation package (VASP) code. Geometry relaxations of the bulk structures of silver, gold, and copper using different XC functionals yielded the respective lattice constants (see Table S1 in the supplementary material for calculated lattice constants compared to the experimental zero-point phonon corrected lattice constants).[75] Since a study by Carter *et al.*[76] showed a non-negligible interaction of the adsorbate molecule with its periodic image for a relatively smaller (3 × 3) supercell, we opted to build a (4 × 4) supercell of (111) surfaces in the atomic simulation environment (ASE)[77,78] using the optimized lattice constants. The supercell has a five-atomic-layer thickness. A vacuum of 12 Å was added along the z-direction to prevent the interactions due to the periodic images. The positions of the atoms on the bottom three layers were fixed during the relaxation to reduce the computational cost. Benzene and thiophene constructed using the reference C–S, C–C, and C–H bond lengths[79,80] were allowed to relax in the slab whose size was identical to that of the surface on which the adsorption occurred. Initially, both thiophene and benzene were placed in a parallel orientation 3 Å above the top metal layer and allowed to relax on the high symmetry sites (fcc, hcp, ontop, and bridge).[77,78] Those sites

were defined using the center of mass and the azimuthal angle of the molecule, as proposed by Liu *et al.*[47] For example, hcp-45 indicates the center of mass of thiophene adsorbed at the hcp site with a symmetry axis rotated by 45° from the direction of metal rows. The surface, the molecule, and the molecule–surface system were all separately relaxed. We followed a similar procedure for the adsorption of xenon (Xe) over the (111) surfaces of Ag and Cu, as well. We used the VASP recommended PAW pseudopotentials for all the calculations. While we used a plane-wave cutoff of 650 eV, the smearing parameter (k_BT) of 0.1 eV was utilized, following the first order Methfessel–Paxton scheme. We used 4 × 4 × 1 and 20 × 20 × 20 Monkhorst–Pack meshes for the Brillouin zone sampling of the surface and the bulk, respectively. The use of a denser k-mesh (6 × 6 × 1) does not change the adsorption energy for benzene and xenon on Cu(111) surfaces by more than 11 and 2 meV, respectively (see Table S2 in the supplementary material). Similarly, the effect of the image-induced dipole interaction between our supercells is less than 20 meV for thiophene[50] and less than 4 meV for benzene. Since both adsorption energies and equilibrium distances depend on the adsorption-site, we utilized all major high symmetry sites for PBE+vdW-dZK and SCAN+vdW-dZK calculations. However, we only used the most stable site (hcp-30 for benzene and fcc-45 for thiophene) for the computation from other methods. We calculated the adsorption energy by subtracting the energy of the surface and molecule from the surface–molecule system,

$$E_{ad} = E_{surf+mol} - E_{surf} - E_{mol}. \quad (3)$$

A similar procedure was adopted for calculating the adsorption energy of Xe and graphene over the metallic surfaces, as well.

For DFT+vdW-dZK calculations, we computed the necessary coefficients using Eqs. (2)–(4) from the work of Tao *et al.*[72] (see Ref. 72 and references therein for more details). We took the necessary parameters of transition metals required for vdW-dZK calculations from the previous work.[72,73] We utilized the experimental static dipole polarizabilities reported in the NIST[81] database for all studied atoms and molecules (see Tables S3–S5 in the supplementary material for the computed coefficients for xenon and renormalized atoms in benzene and thiophene and see Refs. 50, 72, and 73 for details on those coefficients). Finally, we computed the total adsorption energy at each distance by adding the adsorption energy from DFT calculations and the corresponding correction obtained from the vdW-dZK model, following the binding-curve approach as in Fig. 1 of Tang *et al.*[73] (see Figs. S1–S8 in the supplementary material for the computed adsorption energies for benzene, thiophene, and Xe over the (111) surfaces of coinage metals using PBE+vdW-dZK and SCAN+vdW-dZK). The binding energy curve for graphene on Cu(111), Ni(111), and Co(0001) surfaces computed using SCAN metaGGA were taken from the work of Peng *et al.*[62] For graphene on Al(111) surfaces, we computed the binding energy curve using SCAN metaGGA by following the approach of Tang *et al.*[73] The coefficients and parameters required for the vdW-dZK calculations on these systems were taken from Ref. 73 (see Figs. S9 and S10 in the supplementary material for the computed adsorption energies and distances). For PBE+vdW-dZK, the cutoff parameter b is 3.3 bohrs, determined by minimizing the mean absolute error (MAE) between calculated and RPA binding energies of graphene over the transition metal surfaces.[72,73] The goal of our present work is to address the adsorption energies and distances of aromatic molecules on coinage metal surfaces. Due to the availability of the precise experimental adsorption energies for benzene on (111) surfaces of coinage metals,[46] we utilized b = 4.1 bohrs for SCAN+vdW-dZK, based on the least deviation between the calculated and experimental adsorption energies of benzene on these surfaces. In Sec. III D, we show that this choice of the b parameter for SCAN+vdW-dZK also predicts adsorption energies and distances of graphene over transition metals, closer to the RPA values.

III. RESULTS AND DISCUSSION

We have assessed the adsorption energies, the vertical adsorption distances, and the tilt angles of benzene and thiophene placed

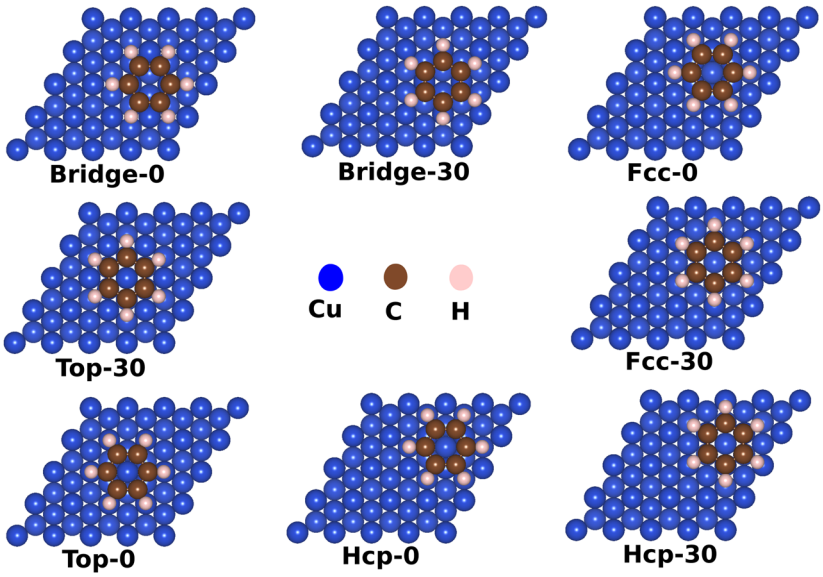

FIG. 1. High symmetry sites[77] utilized for the initial adsorption of a benzene molecule over the (111) surface of copper.

over the (111) surfaces of Cu, Ag, and Au (coinage metals) using the scheme based on the physisorption model (vdW-dZK)[72] following Zaremba–Kohn theory. Currently, this scheme[72] has been implemented to PBE[36] (PBE+vdW-dZK[50,73]), and very recently, the modified[74] form of that scheme has been implemented to SCAN metaGGA. In this work, we are implementing the original scheme[72] (without any modifications) to SCAN[51] (SCAN+vdW-dZK). For comparative purposes, we also paired the semi-local functionals with the non-local functional (rVV10[23]) or the D3[66] method. The common goal of all these methods is to capture the van der Waals (vdW) interaction that is very relevant for the adsorption process but is missing in the bare semi-local functionals. We utilized the parameters of Peng *et al.*[62] based on fitting to binding energy curves of the argon-dimer obtained from CCSD(T) calculations to pair rVV10 with SCAN. In our previous work,[50] we followed the same approach to determine the parameters required to combine rVV10 with PBE, PBEsol, and revSCAN. Finally, the parameters obtained from Brandenburg *et al.*[82] were utilized to combine SCAN with D3 (SCAN+D3).

A. Benzene over Cu(111), Ag(111), and Au(111)

We utilized eight different high symmetry sites for the adsorption of benzene over the (111) surfaces of Cu, Ag, and Au, as displayed in Fig. 1. Our calculations with PBE+vdW-dZK and SCAN+vdW-dZK, in agreement with Liu *et al.*,[47] show a weak dependence of adsorption energy on the site as the maximum energy difference between them is just 0.05 eV. In agreement with past studies,[47,48,62,83] these methods, irrespective of the substrate metals, predict the hollow site (hcp-30) as the most stable site of adsorption. For better comparison, we focused on the most stable site (hcp-30) for all other methods utilized in our work.

In agreement with the experiments,[84–86] all the methods discussed here including PBE+vdW-dZK and SCAN+vdW-dZK predict benzene to adsorb flat (parallel) to the metal surface without any noticeable tilting.

Table I displays the adsorption energy of benzene over the (111) surface of different metal substrates at the most stable site of adsorption. The experimental adsorption energies reported are acquired from the analysis of the data obtained from the temperature-programmed desorption (TPD) measurements. The most commonly used technique is the Redhead analysis,[87] which treats desorption temperature to be independent of the coverage and uses a frequency parameter often guessed over a range of values [$(10^{12}-10^{15})$ s^{-1}]. However, the TPD measurements display a correlation between the coverage and the desorption temperature, questioning the Redhead's analysis. A recent experimental study[46] utilizes the so-called complete analysis,[88] where the frequency factors are determined uniquely for a given coverage. This experiment[46] benchmarks the adsorption energy for benzene adsorbed (within an error bar of 0.05 eV) on the (111) surface of the coinage metals, enabling one to test the accuracy of theoretical methods.

PBE largely underestimates the adsorption energies due to its inability to capture the vdW interaction beyond short-range. SCAN by design can incorporate some intermediate-range interaction, but as evident in our calculations, these are still not sufficient to fully account for the missing long-range vdW interaction. Non-local correlation functionals such as rVV10,[23] VV10,[22] and vdW-DFs[20,21] can often be paired with semilocal (SL) density functional approximations (DFAs) to incorporate such missing interaction. However, our work suggests that the rVV10-based methods are inconsistent due to their over-flexibility in pairing with the base functionals. We will elaborate more on this puzzle in Sec. III E. There are alternative empirical ways to include vdW interactions such as the popular method DFT+D3,[65,66] known for identifying the local chemical environment through improved C_6 coefficients. These methods, in comparison to their predecessors,[63,64] are much more accurate for interaction energies of molecular systems such as the S22 dataset and rare-gas dimers. However, in agreement with the previous work,[45] we found overestimated adsorption energies with these methods. Since the effect of surface metal atoms screening the molecule–surface interaction is ignored even in these improved C_6 coefficients, it could be the major reason behind the poor performance of these methods for our systems. In the DFT+vdW[31] method, the C_6 coefficients along with the vdW radii are determined using the electron density obtained from the base functionals and are independent of these underlying base functionals. However, like DFT+D, this method also lacks screening effects, leading to significantly overestimated[89] adsorption energies. The method DFT+vdW^{surf}[32] was introduced to include the screening effects in DFT+vdW following Lifshitz–Zaremba–Kohn[90,91] theory. Here, the screening effects were included using modified C_6 coefficients rather than explicitly using the C_3 coefficients pertinent for particle–slab interaction. PBE+vdW^{surf} predicted better[63] adsorption energies compared to PBE+vdW,[89] but still the overestimation was noticeable. Another approximation, the DFT+MBD,[33] was introduced to incorporate the screening effects in DFT+vdW. This method reported better adsorption energies[46] when combined with a hybrid functional

TABLE I. Adsorption energy (in eV) of benzene (C_6H_6) when placed on the most stable site (hcp-30) over the (111) surfaces of coinage metals using the different methods. The results from various previous studies are also reported here for comparison.

	C_6H_6/Cu(111)	C_6H_6/Ag(111)	C_6H_6/Au(111)
PBE	−0.06	−0.06	−0.06
PBE+rVV10	−0.58	−0.54	−0.60
PBE+D3	−1.00	−0.86	−0.93
PBE+vdW-dZK	−0.56	−0.60	−0.67
PBE+vdW[89]	−1.07	−0.87	−0.84
PBE+vdW^{surf}[63]	−0.86	−0.75	−0.74
PBE+MBD[46]	−0.63	−0.57	−0.56
PBE+XDM[44]	−0.54	−0.58	−0.61
B86bPBE+XDM[44]	−0.59	−0.68	−0.64
optPBE+vdw-DF[43]	−0.68	−0.71	−0.71
SCAN	−0.43	−0.40	−0.42
SCAN+rVV10	−0.78	−0.75	−0.80
SCAN+D3	−0.93	−0.81	−0.86
SCAN+vdW-dZK	−0.63	−0.60	−0.65
revSCAN+rVV10	−1.11	−0.93	−1.03
HSE+MBD[46]	−0.78	−0.68	−0.67
Expt.[46]	−0.68 ± 0.04	−0.63 ± 0.05	−0.71 ± 0.03

(HSE). However, using a hybrid base functional is computationally demanding. Similarly, the method PBE+XDM,[44] based on the exchange–hole dipole moment,[24,26] reports slightly underestimated adsorption energies. In Table I, we show the results from other important methods from previous studies,[44,46,63,89] as well.

Among all reported methods, SCAN+vdW-dZK stands out. The adsorption energies of benzene over different metal substrates predicted from this method lie close to the error bars of the reported reference values. In Fig. 2, we show the absolute deviation between the reference and calculated adsorption energies using different methods utilized in our work. Despite slightly underbinding benzene on a copper surface, PBE+vdW-dZK lies closest to the reference values for the other two metal surfaces (see Figs. S1–S3 in the supplementary material for the details on PBE+vdW-dZK and SCAN+vdW-dZK calculations). We note here that SCAN+vdW-dZK is designed such that it performs better for the adsorption energies of benzene over coinage metals. The fact that PBE+vdW-dZK also predicts the adsorption energies close to SCAN+vdW-dZK and both closer to the available experimental values indicates the consistency of these methods. Similar conclusions were drawn in the case of adsorption energies of graphene over layered materials,[74] too. Recently, Chowdhury *et al.*[92] extended the vdW-dZK model to address the adsorption of molecules on carbon nanotubes, which have curved cylindrical surfaces. The binding energies calculated from PBE+vdW-dZK and SCAN+vdW-dZK are very close to each other. It further confirms the consistency of the vdW-dZK model.

Finally, based on the molecular orbital density of states (MODOS) analysis by Jiang *et al.*,[63] the d-band center for benzene on Ag(111) lies farther away from the Fermi-level than for benzene on the Au(111) surface. From the perspective of d-band center theory,[93–95] this means that Au(111) should be more reactive than Ag(111) for benzene. The experimental adsorption energies obtained from the so-called complete analysis of TPD measurements support this prediction of d-band center theory too. In this regard, SCAN+vdW-dZK and PBE+vdW-dZK both appear to be qualitatively accurate as well. Although the adsorption energies predicted from methods such as PBE+MBD, HSE+MBD, and optPBE+vdW-DF were reasonable, all those methods predict almost equal adsorption energies of benzene on Ag(111) and Au(111) against the trend predicted by the experiment and the d-band center theory.

Although adsorption energies over different metallic surfaces are close to each other, Reckien *et al.*[45] argued that the vertical adsorption distances are similar for Ag(111) and Au(111) while relatively shorter for Cu(111). This ordering of adsorption distances is consistent with the similar vdW radii of Ag and Au, both being larger than that of Cu. To the best of our knowledge, we have experimental data for the adsorption distance available[96] only for benzene over Ag(111) based on the normal-incidence x-ray standing wave (NIXSW) measurements, as shown in Table II. Although methods such as SCAN+rVV10, PBE+D3, and PBE+rVV10 predict adsorption distances for benzene over Ag(111) closer to the experimental values, they predict similar adsorption distance for different metallic surfaces. SCAN, revSCAN+rVV10, and PBE+vdW-dZK get that order right, but they are quantitatively not close enough to the experimental values. Getting the adsorption distances, orientations, and energies right is a challenge even for most vdW-corrected density functionals as they require a delicate balance between short- and long-range correlations. The popular method optPBE+vdW-DF[43] yields the adsorption energies very close to the experimental values but predicts longer adsorption distances. However, methods such as SCAN+D3[66] predict adsorption distances within the error bar of experimental value yet overestimate the adsorption energies. Very few methods such as B86bPBE+XDM,[44] PBE+vdW^{surf},[46,63] and PBE+MBD[46,63] give a reasonable description of the aforementioned challenges. The orientations and adsorption distances of benzene

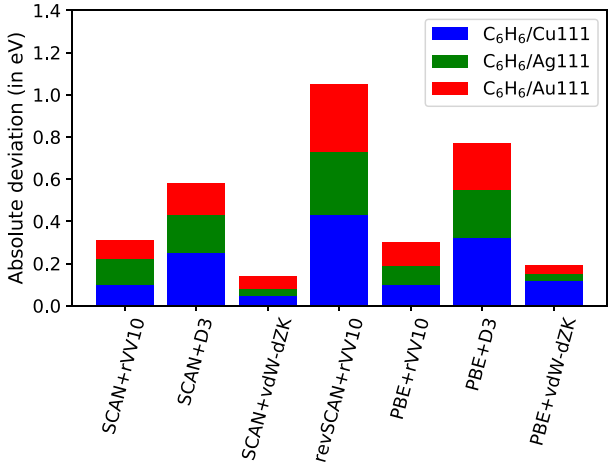

FIG. 2. Absolute deviation between adsorption energies (in eV) of benzene (C_6H_6) on the (111) surfaces of Cu, Ag, and Au calculated using various methods studied in our work and the experimental value obtained from the complete analysis.[88] We note that the uncertainties (not shown in the figure) in the experimental values[46] are ±0.04 eV, ±0.05 eV, and ±0.03 eV for C_6H_6 on the (111) surfaces of Cu, Ag, and Au, respectively.

TABLE II. Adsorption distance (in Å) of the molecule benzene (C_6H_6) when placed on the most stable site (hcp-30) over the (111) surfaces of the coinage metals using different methods. Adsorption distance from various previous studies is also reported here for comparison.

	C_6H_6/Cu(111)	C_6H_6/Ag(111)	C_6H_6/Au(111)
PBE	3.40	3.44	3.42
PBE+rVV10	3.01	3.02	3.01
PBE+D3	2.95	2.97	2.97
PBE+vdW-dZK	3.13	3.23	3.22
PBE+vdW[89]	3.04	3.14	3.21
PBE+vdW^{surf} [63]	2.83	2.97	3.05
B86bPBE+XDM[44]	2.71	3.03	3.15
optPBE+vdw-DF[43]	3.14	3.23	3.21
SCAN	3.01	3.10	3.18
SCAN+rVV10	2.95	2.98	3.01
SCAN+D3	2.90	3.00	2.99
SCAN+vdW-dZK	2.85	3.02	3.06
revSCAN+rVV10	2.66	2.93	2.95
Expt.[96]	...	3.04 ± 0.02	...

over different metallic surfaces predicted by some of the better-performing methods in our work are as shown in Fig. 3. PBE+vdW-dZK is not as impressive for adsorption distances as it was for adsorption energies, but SCAN+vdW-dZK stands out as the best overall performer. Apart from predicting the correct adsorption-sites and orientations of the adsorbate molecule, SCAN+vdW-dZK yields the adsorption energies and distances within the narrow error bar of the available experimental values.

B. Thiophene over Cu(111), Ag(111), and Au(111)

In our previous work,[50] we had demonstrated how the combination of the non-local functional rVV10 combined with metaGGAs failed to deliver for adsorption of the polar molecule thiophene over the (111) surfaces of the coinage metals. We also showed how PBE+vdW-dZK was able to predict adsorption energies, orientations, and distances better than many studied and existing methods. However, in Sec. III A, we showed that the PBE+vdW-dZK predicted adsorption energies of benzene over coinage metals reasonably well but yielded longer adsorption distances, where SCAN+vdW-dZK was reasonable in both areas. Here, we compare the performance of SCAN+vdW-dZK for thiophene over the (111) surfaces of coinage metals.

Experiments[97–99] predict the ontop position of the sulfur atom in the thiophene as the most stable site of adsorption. This site is close to the fcc-45[77] site of the center of the aromatic ring of the thiophene. Based on the given coverage, SCAN+vdW-dZK, in agreement to PBE+vdW-dZK, SCAN+rVV10, revSCAN+rVV10, PBE+rVV10, and PBEsol+rVV10, predicts this fcc-45 site as the most stable site of adsorption.

While experiments[98,100,101] demonstrate thiophene to lie flat over the (111) surfaces of Ag and Au, strong coverage dependent tilting is found[97] over the Cu(111) surface increasing from an angle $12^\circ \pm 2^\circ$–$25^\circ \pm 4^\circ$, when the coverage varies from 0.03 Ml to 0.1 Ml. Most of the theoretical studies[44,50,102] predict thiophene to lie flat even over the Cu(111) surface. SCAN+vdW-dZK, in agreement with the experiments, predicts the flat orientation of thiophene over Ag(111) and Au(111). However, the predicted tilting angle of 7° over Cu(111) is slightly less than the tilt angles observed for 0.03 Ml coverage. Similar tilting was predicted by PBE+vdW^{surf}.[103] Although the tilting angle predicted by PBE+vdW-dZK[50] is close to the values demonstrated by the experiment, Maurer *et al.*,[103] argued that the tilting angles predicted by experiment at finite temperature is larger due to the anharmonicity of the adsorbate-substrate bond.

Table III displays the sulfur–substrate distance (in Å) and the adsorption energy (E_{ad}) (in eV) of thiophene over different substrate metals. The experimental adsorption energies are obtained from the Redhead analysis[87] of the TPD measurements[97,101,105] using 10^{13} s^{-1} as the frequency parameter. We note that for a given TPD measurement, the choice of frequency parameter from 10^{12}–10^{15} s^{-1} can lead to differences up to 0.2 eV. Since thiophene is a small molecule, our choice of frequency parameter, we believe, is a reasonable one. We also note that this frequency parameter is consistent with the choice made by Christian *et al.*[44] for Redhead analysis on similar work. Unfortunately, we have the substrate–sulfur distance available only for thiophene on Cu(111) based on S K-edge x-ray-absorption fine structure measurements.[104,106] In Fig. 4, we display the absolute deviation of the adsorption energies predicted by various methods in our work from the experimental values[97,101,105] obtained using the Redhead analysis.[87] While popular methods such as PBE+D2[102] overestimate E_{ad} and predict shorter distances, methods such as B86bPBE+XDM[44] and PBE+rVV10[50] predict reasonable adsorption energies but yield longer distances. PBE+vdW-dZK predicts the substrate–sulfur distance for thiophene over Cu(111) closer to the experimental value, but it slightly underestimates the adsorption energies. SCAN+vdW-dZK, though it slightly overestimates the adsorption energy of thiophene on Ag(111), is the best overall performer (see Figs. S4–S6 in the supplementary material for the details

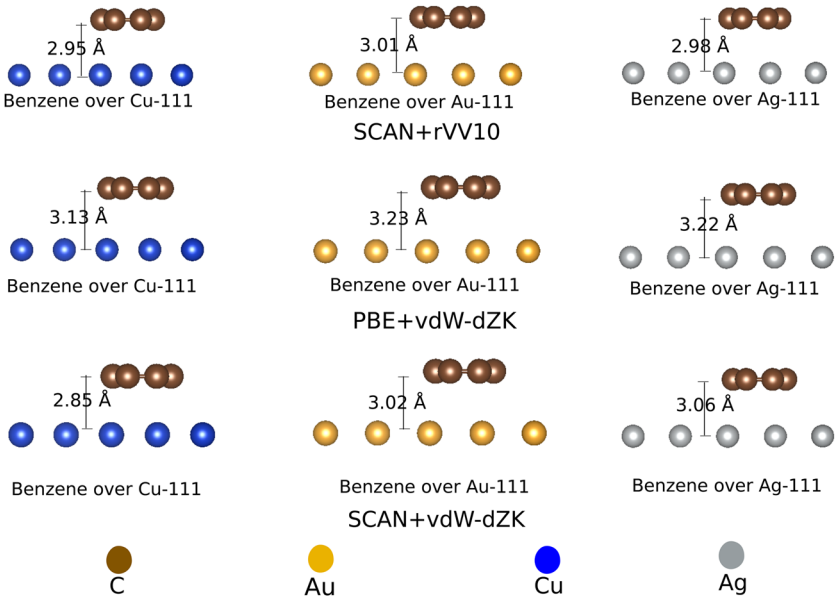

FIG. 3. Adsorption distance of benzene over the (111) surfaces of Cu, Ag, and Au when placed at the most stable site (hcp-30). For convenience, only the results of the three better performers, namely, PBE+vdW-dZK, SCAN+vdW-dZK, and SCAN+rVV10, are displayed.

TABLE III. Substrate–sulfur distance (in Å) and adsorption energy (in eV) of thiophene placed on the most stable site (fcc-45) over the (111) surfaces of the coinage metals using different methods.

	C_4H_4S/Cu(111)		C_4H_4S/Ag(111)		C_4H_4S/Au(111)	
	d(Cu–S)	E_{ad}	d(Ag–S)	E_{ad}	d(Au–S)	E_{ad}
PBE+rVV10[50]	2.88	−0.61	3.00	−0.55	2.98	−0.63
PBE+vdW^{surf}[103]	2.78	−0.82	3.17	−0.72	2.95	−0.77
PBE+D2[102]	2.40	−0.81	...	...	2.75	−1.24
PBE+vdW-dZK[50]	2.57	−0.60	3.16	−0.50	3.23	−0.56
B86bPBE+XDM[44]	2.99	−0.62	3.04	−0.67	2.99	−0.66
PBEsol+rVV10[50]	2.19	−1.22	2.68	−0.93	2.59	−1.06
SCAN+vdW-dZK	2.66	−0.69	3.00	−0.62	2.98	−0.69
Expt.	2.62 ± 0.03[104]	−0.66[97]	...	−0.52[101]	...	−0.68[105]

of SCAN+vdW-dZK calculations). Figure 5 displays the orientation and sulfur–adsorbate distance of thiophene over the (111) surfaces of coinage metals for the three better-performing methods.

C. Xenon (Xe) over Cu(111) and Ag(111)

As a further test of the vdW-dZK model, we assessed the adsorption energy and distance of Xe over the (111) surfaces of Cu and Ag. The binding of Xe with the substrate metal surfaces is a typical physisorption case dominated by vdW interaction. We compare the results from the vdW-dZK methods to the adsorption energies and distances reported by other existing vdW-corrected methods in Table IV. The experimental values tabulated here are from the so-called best estimate[107] and the review work of Diehl *et al.*[108] (see the references therein for more details on experimental results). Although all reported methods agree to the ontop site as the most stable adsorption-site, they predict significantly different adsorption energies and distances. While SCAN without any vdW correction gives the best estimate of the adsorption distances, it significantly underestimates the adsorption energies. In contrast, the non-local correlation functional vdW-DF gives a better description of adsorption energies but yields longer adsorption distances.[110] Although the performance of PBE+vdW is mixed, PBE+vdW^{surf} gives a reasonable estimate of both adsorption energies and distances.[109] While PBE+vdW-dZK performs on similar lines with PBE+vdW^{surf} for the adsorption energy of Xe over Cu(111), it gives a slightly overestimated value of the adsorption energy for Xe over Ag(111). PBE+vdW-dZK predicts slightly shorter adsorption distances for Xe over both the surfaces as well. Although PBEsol+rVV10 s[49] performs better than the most methods discussed here, SCAN+vdW-dZK stands out overall by predicting both adsorption energies and equilibrium distances closer to the error bars of the available experimental values[107,108] (see Figs. S7 and S8 in the supplementary material for the details on PBE+vdW-dZK and SCAN+vdW-dZK calculations).

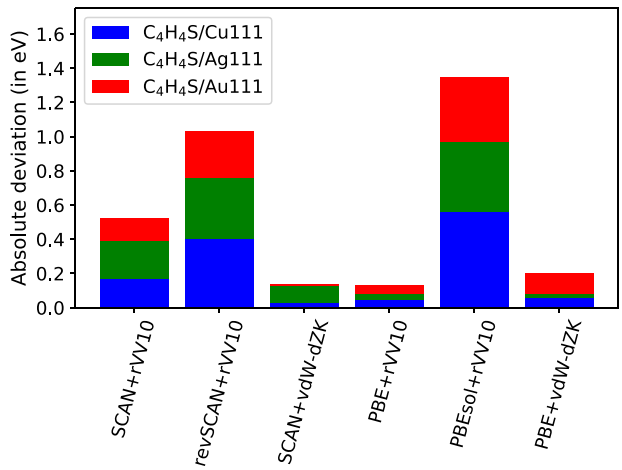

FIG. 4. Absolute deviation between adsorption energies (in eV) of thiophene (C_4H_4S) on the (111) surfaces of Cu, Ag, and Au calculated using various methods studied in our work and the experimental value[97,101,105] obtained using the Redhead Analysis.[87]

D. Graphene over Al(111), Ni(111), Co(0001), and Cu(111)

So far, we have assessed the performance of vdW-dZK methods based on the adsorption of organic molecules and a rare-gas atom on the surfaces of coinage metals. Although the fitting approaches to combine PBE and SCAN to the vdW-dZK model were different, we show that both these vdW-methods give reasonable adsorption energies and distances for benzene, thiophene, and xenon on coinage metals. As a further test of SCAN+vdW-dZK on adsorption of different systems on different metal surfaces, we assessed the binding energies and distances of a graphene sheet on Al(111), Ni(111), Co(0001), and Cu(111). Those metal surfaces were also used to determine the fit parameter for PBE+vdW-dZK.[72,73] This set consists of at least one representative of simple sp-metal (Al), coinage metal with completely filled d-bands (Cu), and transition metals with partially filled d-bands (Ni and Co). In Table V, we show the SCAN+vdW-dZK results along with those of PBE+vdW-dZK and RPA.

SCAN+vdW-dZK systematically underestimates the RPA binding energies with a mean absolute error (MAE) of about

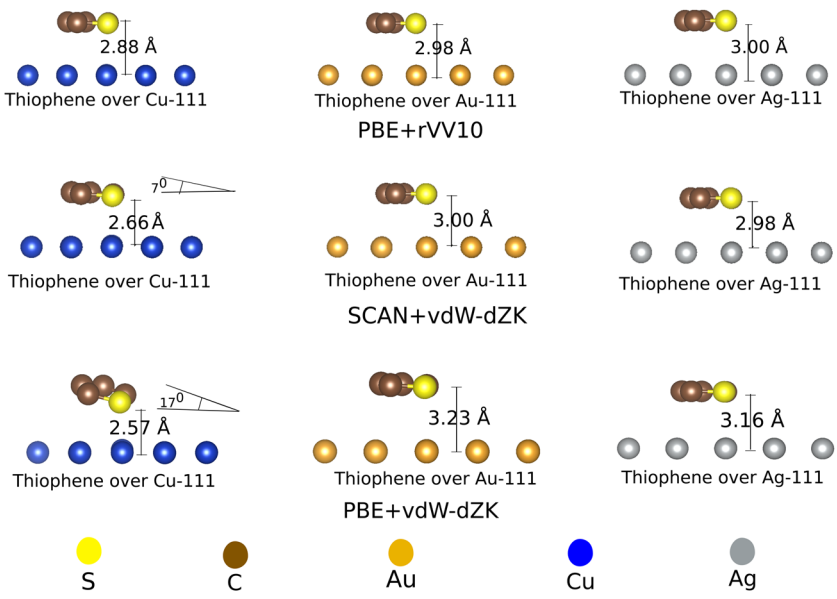

FIG. 5. Adsorption distance and tilt angle of thiophene over the (111) surfaces of Cu, Ag, and Au placed at the most stable site of adsorption (fcc-45). For convenience, the results of the three better performers, namely, PBE+vdW-dZK, SCAN+vdW-dZK, and PBE+rVV10, are shown.

11 meV/C atom. This value is slightly higher than that predicted by PBE+vdW-dZK. However, for the equilibrium distances, SCAN+vdW-dZK predictions are closer to RPA than those of PBE+vdW-dZK. Remarkably, SCAN+vdW-dZK performs on par with PBE+vdW-dZK for the systems that parameterize PBE+vdW-dZK. More importantly, they both are close to the reference values whenever available.

In our previous work,[50] we demonstrated the ability of PBE+vdW-dZK to predict reasonable adsorption energies and distances of relatively large-sized molecules such as PTCDA on Ag(111), as well. We note that there are many molecules of diverse size and polarity that can show more complex interactions with the substrate metal atoms, and addressing all of them can be challenging for any theoretical model. However, the test for vdW-dZK methods for the adsorption of small prototype molecules such as benzene and thiophene on coinage metals shows encouraging results.

TABLE IV. Xe–substrate distance (in Å) and adsorption energy (in meV) of Xe placed on the most stable site (ontop) over Ag(111) and Cu(111).

	Xe/Cu(111)		Xe/Ag(111)	
	E_ad	d(Xe–Cu)	E_ad	d(Xe–Ag)
PBE	−21	4.25	−21	4.27
PBE+vdW[109]	−335	3.48	−244	3.60
PBE+vdW^{surf}[109]	−248	3.46	−237	3.57
PBE+vdW-dZK	−252	3.29	−275	3.37
PBEsol +rVV10 s[49]	−165	3.5	−186	3.4
vdW-DF[110]	−184	3.97	−180	4.08
vdW-DF2[110]	−157	4.01	−154	4.00
SCAN	−90	3.61	−93	3.57
SCAN +vdW-dZK	−187	3.47	−197	3.49
Expt.[107,108]	−(183 ± 10)	3.60 ± 0.08	−(211 ± 15)	3.60 ± 0.05

E. Performance of the rVV10-based methods

In our present study, we utilized a nonlocal correlation functional rVV10[23] paired with PBE, PBEsol, SCAN, and revSCAN to include the long-range vdW effects required for the accurate description of the organic molecule adsorbed over the metallic surfaces. We noted a strong discrepancy in the description of the molecule–metal system between different rVV10-based methods. While PBE+rVV10 slightly underestimates the adsorption energies for benzene, it gives a reasonable description in the case of thiophene. SCAN+rVV10 overestimates in the case of adsorption of both molecules. Some recent studies[60,74] suggest SCAN+rVV10 to be overestimating in general. When combined with revSCAN,[61] rVV10 is significantly overestimating the adsorption energies of those molecules over the metallic surfaces. Although revSCAN[61] was designed to remove the intermediate-range interactions of SCAN, when paired with rVV10, it proved to be over-correcting. PBEsol+rVV10 yields almost double the adsorption energies of thiophene over metallic surfaces compared to PBE+rVV10.[50] However, rVV10 is not the only nonlocal functional to demonstrate such strong dependence on the base functional to which it combines. A noticeable dependence on base functionals was reported for nonlocal correlation functionals such as vdW-DFs,[20,21] as well. When the revPBE[37] base functional proposed for vdW-DF[20] was replaced by the revised version[111] of PW86[112] for vdW-DF2,[21] it yielded better accuracy for molecular complexes. While both these base functionals[43] underestimated the adsorption energies for benzene on coinage metals, the pairing with less repulsive base functionals[39] such as optPBE and optB88 gave a better description.

rVV10, unlike vdW-DFs, is much more flexible to pair with the base functional and does so with a set of parameters, namely, "b" and "C." The former controls the short-range damping, while

TABLE V. Graphene–substrate distance (in Å) and adsorption energy (in meV per C atom) of graphene over Cu(111), Ni(111), Co(0001), and Al(111). The RPA and PBE+vdW-dZK values are reported from the work of Tang *et al.*[73]

	Graphene–substrate distance			Adsorption energy per C atom		
	RPA	PBE +vdW-dZK	SCAN +vdW-dZK	RPA	PBE +vdW-dZK	SCAN +vdW-dZK
Gr/Cu(111)	3.09	3.56	3.24	−68	−65	−56
Gr/Ni(111)	3.26	3.29	3.25	−70	−69	−58
Gr/Co(0001)	3.25	3.56	3.27	−66	−58	−55
Gr/Al(111)	3.51	3.6	3.64	−52	−73	−42
MAE		0.23	0.08		8	11

the latter controls the accuracy of the C_6 coefficient at large separation. Most studies regarding parameterization[23,48,50,62] of rVV10 keep the value of "C" equal to 0.0093 fixed as originally proposed by Vydrov *et al.*,[22] as changing "C" does not significantly change the binding curve.[62] Therefore, it is usually a single parameter "b" that defines the pairing. Determination of this parameter requires fitting to well-benchmarked systems where the vdW interaction is significant, such as interaction energies of the S22 dataset, the binding energy of rare-gas dimers, and interlayer binding energies of layered materials. However, we noted a significant inconsistency in the performance of the rVV10-based methods when we determined the parameters for a particular base functional from different possible fitting methods. It is a more serious problem as this creates enough doubts over which parameterization to choose for combining rVV10 to a particular base functional for the particular problem. Fortunately, for SCAN+rVV10,[62] the "b" parameter obtained from fitting to the binding energy of rare-gas dimers produced fewer errors for other systems as well. The "b" parameter for PBE+rVV10 is 6.6 and 10.0 when fitted to the interaction energies of the S22 data set and interlayer binding energies of the layered materials, respectively.[48] However, both these values are different (b = 9.7) from the parameter obtained by fitting to the argon-dimer binding energy.[50] In our previous work,[50] we obtained b = 9.7 for PBEsol+rVV10 using the argon-dimer parameterization, which is significantly different from b = 20 based on fitting to the interlayer binding energy of layered materials.[49] The latter choice of the parameter significantly underperformed for binding energies of the argon-dimer compared to the former and was also unsatisfactory for interaction energies of the S22 dataset compared to PBE+rVV10 (b = 6.6) and SCAN+rVV10.

TABLE VI. Comparison of adsorption energies (in eV) of PBE+rVV10 and PBEsol+rVV10 based on separate parameterizations using the S22 dataset, Ar_2 binding energies, and interlayer binding energies of layered materials (LM) for thiophene adsorbed on the (111) surface of coinage metals.

		PBE+rVV10		PBEsol+rVV10	
	References	Ar_2	S22	Ar_2	LM
Cu	−0.66[97]	−0.61	−0.95	−1.22	−0.75
Au	−0.68[105]	−0.63	−0.94	−1.06	−0.69
Ag	−0.52[101]	−0.55	−0.82	−0.93	−0.59

In Table VI, we compare the adsorption energy of thiophene over the coinage metals, at the most stable site (fcc-45), from the different parameterization of rVV10 for PBE or PBEsol. We observed significant differences in the adsorption energies when different parameterizations combined rVV10 to the same base functional, illustrating the inconsistency in the performance of rVV10-based methods. The need for an improved two-parameter damping function of rVV10 is being explored by Tang, Chowdhury, and Perdew,[113] and it would hopefully solve larger parts of this problem.

IV. CONCLUSION

In this work, we investigated the geometry and energetics of the adsorption of xenon and two widely studied prototype molecules, namely, benzene and thiophene, over the (111) surface of the coinage metals using density functional theory (DFT).

Recently, the so-called complete analysis method[88] was used to analyze the temperature-programmed desorption (TPD) measurement of benzene over coinage metal surfaces[46] yielding adsorption energies within an error bar of chemical accuracy (0.04 eV). Based on our results, the recently introduced model based on Zaremba–Kohn's second-order perturbation theory (DFT+vdW-dZK) predicts the adsorption energies of benzene over metal surfaces better than any other methods reported here. In particular, SCAN+vdW-dZK stands out. Apart from yielding the correct orientation and site, this method predicts the energies and distances within the error bar of the experiment. SCAN+vdW-dZK predicts Au(111) to be more reactive than Ag(111), supporting the popular d-band center theory. SCAN+vdW-dZK is the best overall performer for xenon and thiophene over metallic surfaces, as well. We note that due to the unavailability of the results from the complete analysis, Readhead's analysis,[87] which is also widely used but not as accurate as of the former, was utilized here to analyze the TPD measurements of thiophene adsorbed over the metallic surfaces. We also assessed the adsorption energies and distances of graphene adsorbed on four diverse metallic surfaces and showed that the vdW-dZK methods display reasonable agreement with the available RPA reference values.

Finally, through the example of thiophene adsorbed on metal surfaces, we demonstrate that the rVV10-based methods are inconsistent. They predict significantly different adsorption energies of a molecule–metal system when the same base-functional pairs with

rVV10 through different possible parameterizations. The current rVV10 is essentially a pairwise form in which the screening effects of metal substrates are not included explicitly in the molecule–metallic surface interactions. The vdW-dZK model incorporates such screening effects explicitly via the C_3 and C_5 nonlocal terms, making the model more accurate to describe the molecule–metallic surface interactions. Although the vdW-dZK model combines with PBE or SCAN through a single parameter (b), this model relies on the accurate static dipole polarizabilities as an input parameter. In the current implementation, this model only makes post-corrections to the binding energy curve obtained from DFT calculations without relying on the calculated local densities. That limits the applicability of these methods to study the variation on charge transfer or any other density-related properties arising due to the inclusion of vdW interaction in the system. In our present work, we show that SCAN+vdW-dZK is slightly better than PBE+vdW-dZK on the overall performance. The adsorption distances predicted by SCAN+vdW-dZK show better agreement with the experimental values compared to PBE+vdW-dZK. However, there are no significant differences in the adsorption energies predicted by these methods. Despite the vdW-dZK methods combining with two different functionals PBE and SCAN, it is remarkable that the adsorption energies both these methods predict are close to each other, and importantly, both close to the experimental values. Finally, we note that several molecules can show more complex interactions with the substrate metal atoms. Although it is encouraging that these vdW-dZK methods perform well for adsorption of graphene, rare-gas atoms, and two prototype organic molecules, further tests are needed to verify the transferability of these methods to broader adsorbate–adsorbent interactions.

SUPPLEMENTARY MATERIAL

See the supplementary material for computed lattice constants, **k**-point convergence results, coefficients required for vdW-dZK calculations, and the resulting binding energy curves.

ACKNOWLEDGMENTS

S.A. and A.R. acknowledge the support of the U.S. Department of Energy, Office of Science, Office of Basic Energy Sciences, as part of the Computational Chemical Sciences Program under Award No. DE-SC0018331. H.T. acknowledges support from the DOE Office of Science, Basic Energy Sciences (BES), the U.S. Department of Energy, under Grant No. DE-SC0018194. The work of N.K.N. was supported by the National Science Foundation (NSF) under Grant No. DMR-1553022. This research includes calculations carried out on HPC resources supported, in part, by the NSF through major research instrumentation under Grant No. 1625061 and by the U.S. Army Research Laboratory under Contract No. W911NF-16-2-0189. We thank Professor John P. Perdew for his valuable help throughout.

DATA AVAILABILITY

The data that support the findings of this study are available within the article and its supplementary material.

REFERENCES

[1] Q. He, S. Wu, Z. Yin, and H. Zhang, "Graphene-based electronic sensors," Chem. Sci. **3**, 1764–1772 (2012).
[2] F. Yavari and N. Koratkar, "Graphene-based chemical sensors," J. Phys. Chem. Lett. **3**, 1746–1753 (2012).
[3] Á. Logadóttir, P. G. Moses, B. Hinnemann, N.-Y. Topsøe, K. G. Knudsen, H. Topsøe, and J. K. Nørskov, "A density functional study of inhibition of the HDS hydrogenation pathway by pyridine, benzene, and H_2S on MoS_2-based catalysts," Catal. Today **111**, 44–51 (2006).
[4] P. G. Moses, B. Hinnemann, H. Topsøe, and J. K. Nørskov, "The effect of co-promotion on MoS_2 catalysts for hydrodesulfurization of thiophene: A density functional study," J. Catal. **268**, 201–208 (2009).
[5] N. Koch, N. Ueno, and A. T. S. Wee, *The Molecule-Metal Interface* (John Wiley & Sons, 2013).
[6] M. Oehzelt, N. Koch, and G. Heimel, "Organic semiconductor density of states controls the energy level alignment at electrode interfaces," Nat. Commun. **5**, 4174 (2014).
[7] G. Witte and C. Wöll, "Growth of aromatic molecules on solid substrates for applications in organic electronics," J. Mater. Res. **19**, 1889–1916 (2004).
[8] C. M. Friend and D. A. Chen, "Fundamental studies of hydrodesulfurization by metal surfaces," Polyhedron **16**, 3165–3175 (1997).
[9] P. Gomez-Romero, "Hybrid organic–inorganic materials—In search of synergic activity," Adv. Mater. **13**, 163–174 (2001).
[10] A. Tkatchenko, L. Romaner, O. T. Hofmann, E. Zojer, C. Ambrosch-Draxl, and M. Scheffler, "Van der Waals interactions between organic adsorbates and at organic/inorganic interfaces," MRS Bull. **35**, 435–442 (2010).
[11] W. Liu, A. Tkatchenko, and M. Scheffler, "Modeling adsorption and reactions of organic molecules at metal surfaces," Acc. Chem. Res. **47**, 3369–3377 (2014).
[12] M. Stöhr, T. Van Voorhis, and A. Tkatchenko, "Theory and practice of modeling van der Waals interactions in electronic-structure calculations," Chem. Soc. Rev. **48**, 4118–4154 (2019).
[13] D. Yuan, Y. Zhang, W. Ho, and R. Wu, "Effects of van der Waals dispersion interactions in density functional studies of adsorption, catalysis, and tribology on metals," J. Phys. Chem. C **124**, 16926–16942 (2020).
[14] P. Hohenberg and W. Kohn, "Inhomogeneous electron gas," Phys. Rev. **136**, B864 (1964).
[15] W. Kohn and L. J. Sham, "Self-consistent equations including exchange and correlation effects," Phys. Rev. **140**, A1133 (1965).
[16] R. O. Jones, "Density functional theory: Its origins, rise to prominence, and future," Rev. Mod. Phys. **87**, 897 (2015).
[17] J. P. Perdew and K. Schmidt, "Jacob's ladder of density functional approximations for the exchange-correlation energy," AIP Conf. Proc. **577**, 1–20 (2001).
[18] J. F. Dobson, J. Wang, B. P. Dinte, K. McLennan, and H. M. Le, "Soft cohesive forces," Int. J. Quantum Chem. **101**, 579–598 (2005).
[19] H.-V. Nguyen and G. Galli, "A first-principles study of weakly bound molecules using exact exchange and the random phase approximation," J. Chem. Phys. **132**, 044109 (2010).
[20] M. Dion, H. Rydberg, E. Schröder, D. C. Langreth, and B. I. Lundqvist, "Van der Waals density functional for general geometries," Phys. Rev. Lett. **92**, 246401 (2004).
[21] K. Lee, É. D. Murray, L. Kong, B. I. Lundqvist, and D. C. Langreth, "Higher-accuracy van der Waals density functional," Phys. Rev. B **82**, 081101 (2010).
[22] O. A. Vydrov and T. Van Voorhis, "Nonlocal van der Waals density functional: The simpler the better," J. Chem. Phys. **133**, 244103 (2010).
[23] R. Sabatini, T. Gorni, and S. de Gironcoli, "Nonlocal van der Waals density functional made simple and efficient," Phys. Rev. B **87**, 041108 (2013).
[24] A. D. Becke and E. R. Johnson, "A density-functional model of the dispersion interaction," J. Chem. Phys. **123**, 154101 (2005).
[25] E. R. Johnson and A. D. Becke, "A post-Hartree–Fock model of intermolecular interactions," J. Chem. Phys. **123**, 024101 (2005).
[26] A. D. Becke and E. R. Johnson, "A unified density-functional treatment of dynamical, nondynamical, and dispersion correlations," J. Chem. Phys. **127**, 124108 (2007).

[27]S. Grimme, "Accurate description of van der Waals complexes by density functional theory including empirical corrections," J. Comput. Chem. **25**, 1463–1473 (2004).
[28]S. Grimme, "Semiempirical GGA-type density functional constructed with a long-range dispersion correction," J. Comput. Chem. **27**, 1787–1799 (2006).
[29]S. Grimme, J. Antony, S. Ehrlich, and H. Krieg, "A consistent and accurate *ab initio* parametrization of density functional dispersion correction (DFT-D) for the 94 elements H–Pu," J. Chem. Phys. **132**, 154104 (2010).
[30]S. Grimme, S. Ehrlich, and L. Goerigk, "Effect of the damping function in dispersion corrected density functional theory," J. Comput. Chem. **32**, 1456–1465 (2011).
[31]A. Tkatchenko and M. Scheffler, "Accurate molecular van der Waals interactions from ground-state electron density and free-atom reference data," Phys. Rev. Lett. **102**, 073005 (2009).
[32]V. G. Ruiz, W. Liu, E. Zojer, M. Scheffler, and A. Tkatchenko, "Density-functional theory with screened van der Waals interactions for the modeling of hybrid inorganic-organic systems," Phys. Rev. Lett. **108**, 146103 (2012).
[33]A. Tkatchenko, R. A. DiStasio, Jr., R. Car, and M. Scheffler, "Accurate and efficient method for many-body van der Waals interactions," Phys. Rev. Lett. **108**, 236402 (2012).
[34]J. Klimeš and A. Michaelides, "Perspective: Advances and challenges in treating van der Waals dispersion forces in density functional theory," J. Chem. Phys. **137**, 120901 (2012).
[35]S. J. Jenkins, "Aromatic adsorption on metals via first-principles density functional theory," Proc. R. Soc. A **465**, 2949–2976 (2009).
[36]J. P. Perdew, K. Burke, and M. Ernzerhof, "Generalized gradient approximation made simple," Phys. Rev. Lett. **77**, 3865–3868 (1996).
[37]Y. Zhang and W. Yang, "Comment on 'Generalized gradient approximation made simple'," Phys. Rev. Lett. **80**, 890 (1998).
[38]J. P. Perdew, A. Ruzsinszky, G. I. Csonka, O. A. Vydrov, G. E. Scuseria, L. A. Constantin, X. Zhou, and K. Burke, "Restoring the density-gradient expansion for exchange in solids and surfaces," Phys. Rev. Lett. **100**, 136406 (2008).
[39]J. Klimeš, D. R. Bowler, and A. Michaelides, "Chemical accuracy for the van der Waals density functional," J. Phys.: Condens. Matter **22**, 022201 (2009).
[40]A. D. Becke, "Density functional calculations of molecular bond energies," J. Chem. Phys. **84**, 4524–4529 (1986).
[41]A. D. Becke, "Density-functional exchange-energy approximation with correct asymptotic behavior," Phys. Rev. A **38**, 3098 (1988).
[42]A. D. Becke, "On the large-gradient behavior of the density functional exchange energy," J. Chem. Phys. **85**, 7184–7187 (1986).
[43]H. Yildirim, T. Greber, and A. Kara, "Trends in adsorption characteristics of benzene on transition metal surfaces: Role of surface chemistry and van der Waals interactions," J. Phys. Chem. C **117**, 20572–20583 (2013).
[44]M. S. Christian, A. Otero-de-la-Roza, and E. R. Johnson, "Surface adsorption from the exchange-hole dipole moment dispersion model," J. Chem. Theory Comput. **12**, 3305–3315 (2016).
[45]W. Reckien, M. Eggers, and T. Bredow, "Theoretical study of the adsorption of benzene on coinage metals," Beilstein J. Org. Chem. **10**, 1775–1784 (2014).
[46]F. Maaß, Y. Jiang, W. Liu, A. Tkatchenko, and P. Tegeder, "Binding energies of benzene on coinage metal surfaces: Equal stability on different metals," J. Chem. Phys. **148**, 214703 (2018).
[47]W. Liu, V. G. Ruiz, G.-X. Zhang, B. Santra, X. Ren, M. Scheffler, and A. Tkatchenko, "Structure and energetics of benzene adsorbed on transition-metal surfaces: Density-functional theory with van der Waals interactions including collective substrate response," New J. Phys. **15**, 053046 (2013).
[48]H. Peng and J. P. Perdew, "Rehabilitation of the Perdew–Burke–Ernzerhof generalized gradient approximation for layered materials," Phys. Rev. B **95**, 081105 (2017).
[49]A. V. Terentjev, L. A. Constantin, and J. Pitarke, "Dispersion-corrected PBEsol exchange-correlation functional," Phys. Rev. B **98**, 214108 (2018).
[50]S. Adhikari, H. Tang, B. Neupane, A. Ruzsinszky, and G. I. Csonka, "Molecule-surface interaction from van der Waals-corrected semilocal density functionals: The example of thiophene on transition-metal surfaces," Phys. Rev. Mater. **4**, 025005 (2020).
[51]J. Sun, A. Ruzsinszky, and J. P. Perdew, "Strongly constrained and appropriately normed semilocal density functional," Phys. Rev. Lett. **115**, 036402 (2015).
[52]E. B. Isaacs and C. Wolverton, "Performance of the strongly constrained and appropriately normed density functional for solid-state materials," Phys. Rev. Mater. **2**, 063801 (2018).
[53]N. K. Nepal, S. Adhikari, J. E. Bates, and A. Ruzsinszky, "Treating different bonding situations: Revisiting Au-Cu alloys using the random phase approximation," Phys. Rev. B **100**, 045135 (2019).
[54]N. K. Nepal, S. Adhikari, B. Neupane, and A. Ruzsinszky, "Formation energy puzzle in intermetallic alloys: Random phase approximation fails to predict accurate formation energies," Phys. Rev. B **102**, 205121 (2020).
[55]Y. Fu and D. J. Singh, "Applicability of the strongly constrained and appropriately normed density functional to transition-metal magnetism," Phys. Rev. Lett. **121**, 207201 (2018).
[56]J. Sun, R. C. Remsing, Y. Zhang, Z. Sun, A. Ruzsinszky, H. Peng, Z. Yang, A. Paul, U. Waghmare, X. Wu *et al.*, "Accurate first-principles structures and energies of diversely bonded systems from an efficient density functional," Nat. Chem. **8**, 831 (2016).
[57]C. Shahi, J. Sun, and J. P. Perdew, "Accurate critical pressures for structural phase transitions of group IV, III-V, and II-VI compounds from the SCAN density functional," Phys. Rev. B **97**, 094111 (2018).
[58]N. K. Nepal, A. Ruzsinszky, and J. E. Bates, "Rocksalt or cesium chloride: Investigating the relative stability of the cesium halide structures with random phase approximation based methods," Phys. Rev. B **97**, 115140 (2018).
[59]N. K. Nepal, L. Yu, Q. Yan, and A. Ruzsinszky, "First-principles study of mechanical and electronic properties of bent monolayer transition metal dichalcogenides," Phys. Rev. Mater. **3**, 073601 (2019).
[60]J. Yu, G. Fiorin, H. Peng, M. L. Klein, and J. P. Perdew, "Different bonding type along each crystallographic axis: Computational study of poly (*p*-phenylene terephthalamide)," Phys. Rev. Mater. **4**, 055601 (2020).
[61]P. D. Mezei, G. I. Csonka, and M. Kállay, "Simple modifications of the SCAN meta-generalized gradient approximation functional," J. Chem. Theory Comput. **14**, 2469–2479 (2018).
[62]H. Peng, Z.-H. Yang, J. P. Perdew, and J. Sun, "Versatile van der Waals density functional based on a meta-generalized gradient approximation," Phys. Rev. X **6**, 041005 (2016).
[63]Y. Jiang, S. Yang, S. Li, and W. Liu, "Aromatic molecules on low-index coinage metal surfaces: Many-body dispersion effects," Sci. Rep. **6**, 39529 (2016).
[64]A. Takahashi, F. H. Yang, and R. T. Yang, "New sorbents for desulfurization by π-complexation: Thiophene/benzene adsorption," Ind. Eng. Chem. Res. **41**, 2487–2496 (2002).
[65]A.-L. Revelli, F. Mutelet, and J.-N. Jaubert, "Extraction of benzene or thiophene from *n*-heptane using ionic liquids. NMR and thermodynamic study," J. Phys. Chem. B **114**, 4600–4608 (2010).
[66]S. Adhikari, B. Santra, S. Ruan, P. Bhattarai, N. K. Nepal, K. A. Jackson, and A. Ruzsinszky, "The Fermi–Löwdin self-interaction correction for ionization energies of organic molecules," J. Chem. Phys. **153**, 184303 (2020).
[67]G. I. Panov, "Advances in oxidation catalysis; oxidation of benzene to phenol by nutrous oxide," Cattech **4**, 18–31 (2000).
[68]K.-Y. Tsai, I. Wang, and T.-C. Tsai, "Zeolite supported platinum catalysts for benzene hydrogenation and naphthene isomerization," Catal. Today **166**, 73–78 (2011).
[69]L. Foppa and J. Dupont, "Benzene partial hydrogenation: Advances and perspectives," Chem. Soc. Rev. **44**, 1886–1897 (2015).
[70]X. Jia and W. An, "Adsorption of monocyclic aromatics on transition metal surfaces: Insight into variation of binding strength from first-principles," J. Phys. Chem. C **122**, 21897–21909 (2018).
[71]R. J. Angelici, "Heterogeneous catalysis of the hydrodesulfurization of thiophenes in petroleum: An organometallic perspective of the mechanism," Acc. Chem. Res. **21**, 387–394 (1988).
[72]J. Tao, H. Tang, A. Patra, P. Bhattarai, and J. P. Perdew, "Modeling the physisorption of graphene on metals," Phys. Rev. B **97**, 165403 (2018).
[73]H. Tang, J. Tao, A. Ruzsinszky, and J. P. Perdew, "A van der Waals correction to the physisorption of graphene on metal surfaces," J. Phys. Chem. C **123**, 13748 (2019).

[74]H. Tang, J. Tao, J. P. Perdew *et al.*, "Density functionals combined with van der Waals corrections for graphene adsorbed on layered materials," Phys. Rev. B **101**, 195426 (2020).
[75]P. Hao, Y. Fang, J. Sun, G. I. Csonka, P. H. Philipsen, and J. P. Perdew, "Lattice constants from semilocal density functionals with zero-point phonon correction," Phys. Rev. B **85**, 014111 (2012).
[76]D. J. Carter and A. L. Rohl, "van der Waals corrected density functional calculations of the adsorption of benzene on the Cu (111) surface," J. Comput. Chem. **35**, 2263–2271 (2014).
[77]A. H. Larsen *et al.*, "The atomic simulation environment—A python library for working with atoms," J. Phys.: Condens. Matter **29**, 273002 (2017).
[78]S. R. Bahn and K. W. Jacobsen, "An object-oriented scripting interface to a legacy electronic structure code," Comput. Sci. Eng. **4**, 56–66 (2002).
[79]W. R. Harshbarger and S. H. Bauer, "An electron diffraction study of the structure of thiophene, 2-chlorothiophene and 2-bromothiophene," Acta Crystallogr., Sect. B **26**, 1010–1020 (1970).
[80]D. Mootz and H. G. Wussow, "Crystal structures of pyridine and pyridine trihydrate," J. Chem. Phys. **75**, 1517–1522 (1981).
[81]*NIST Computational Chemistry Comparison and Benchmark Database*, NIST Standard Reference Database Number 101 Release 21, edited by R. D. Johnson III (National Institute of Standards and Technology, 2020), http://cccbdb.nist.gov/.
[82]J. Brandenburg, J. Bates, J. Sun, and J. Perdew, "Benchmark tests of a strongly constrained semilocal functional with a long-range dispersion correction," Phys. Rev. B **94**, 115144 (2016).
[83]A. Bilić, J. R. Reimers, N. S. Hush, R. C. Hoft, and M. J. Ford, "Adsorption of benzene on copper, silver, and gold surfaces," J. Chem. Theory Comput. **2**, 1093–1105 (2006).
[84]M. Xi, M. X. Yang, S. K. Jo, B. E. Bent, and P. Stevens, "Benzene adsorption on Cu (111): Formation of a stable bilayer," J. Chem. Phys. **101**, 9122–9131 (1994).
[85]X.-L. Zhou, M. E. Castro, and J. M. White, "Interactions of UV photons and low energy electrons with chemisorbed benzene on Ag (111)," Surf. Sci. **238**, 215–225 (1990).
[86]D. Syomin, J. Kim, B. E. Koel, and G. B. Ellison, "Identification of adsorbed phenyl (C_6H_5) groups on metal surfaces: Electron-induced dissociation of benzene on Au (111)," J. Phys. Chem. B **105**, 8387–8394 (2001).
[87]P. A. Redhead, "Thermal desorption of gases," Vacuum **12**, 203–211 (1962).
[88]D. A. King, "Thermal desorption from metal surfaces: A review," Surf. Sci. **47**, 384–402 (1975).
[89]J. Carrasco, W. Liu, A. Michaelides, and A. Tkatchenko, "Insight into the description of van der Waals forces for benzene adsorption on transition metal (111) surfaces," J. Chem. Phys. **140**, 084704 (2014).
[90]I. M. Lifshitz and A. M. Kosevich, "Theory of magnetic susceptibility in metals at low temperatures," Sov. Phys. -JETP **2**, 636–645 (1956).
[91]E. Zaremba and W. Kohn, "Van der waals interaction between an atom and a solid surface," Phys. Rev. B **13**, 2270 (1976).
[92]S. T. u. R. Chowdhury, H. Tang, and J. P. Perdew, "van der Waals corrected density functionals for cylindrical surfaces: Ammonia and nitrogen dioxide adsorbed on a single-walled carbon nanotube" (unpublished) (2021).
[93]B. Hammer and J. K. Nørskov, "Electronic factors determining the reactivity of metal surfaces," Surf. Sci. **343**, 211–220 (1995).
[94]B. Hammer and J. K. Norskov, "Why gold is the noblest of all the metals," Nature **376**, 238–240 (1995).
[95]B. Hammer and J. K. Nørskov, "Theoretical surface science and catalysis—Calculations and concepts," Adv. Catal. **45**, 71–129 (2000).
[96]W. Liu, F. Maaß, M. Willenbockel, C. Bronner, M. Schulze, S. Soubatch, F. S. Tautz, P. Tegeder, and A. Tkatchenko, "Quantitative prediction of molecular adsorption: Structure and binding of benzene on coinage metals," Phys. Rev. Lett. **115**, 036104 (2015).
[97]P. K. Milligan, B. Murphy, D. Lennon, B. C. C. Cowie, and M. Kadodwala, "A complete structural study of the coverage dependence of the bonding of thiophene on Cu (111)," J. Phys. Chem. B **105**, 140–148 (2001).
[98]G.-J. Su, H.-M. Zhang, L.-J. Wan, and C.-L. Bai, "Phase transition of thiophene molecules on Au (1 1 1) in solution," Surf. Sci. **531**, L363–L368 (2003).
[99]G. B. D. Rousseau, N. Bovet, S. M. Johnston, D. Lennon, V. Dhanak, and M. Kadodwala, "The structure of a coadsorbed layer of thiophene and CO on Cu (111)," Surf. Sci. **511**, 190–202 (2002).
[100]M. H. Dishner, J. C. Hemminger, and F. J. Feher, "Formation of a self-assembled monolayer by adsorption of thiophene on Au (111) and its photooxidation," Langmuir **12**, 6176–6178 (1996).
[101]P. Väterlein, M. Schmelzer, J. Taborski, T. Krause, F. Viczian, M. Bäßler, R. Fink, E. Umbach, and W. Wurth, "Orientation and bonding of thiophene and 2, 2′-bithiophene on Ag (111): A combined near edge extended X-ray absorption fine structure and Xα scattered-wave study," Surf. Sci. **452**, 20–32 (2000).
[102]K. Tonigold and A. Groß, "Adsorption of small aromatic molecules on the (111) surfaces of noble metals: A density functional theory study with semiempirical corrections for dispersion effects," J. Chem. Phys. **132**, 224701 (2010).
[103]R. J. Maurer, V. G. Ruiz, J. Camarillo-Cisneros, W. Liu, N. Ferri, K. Reuter, and A. Tkatchenko, "Adsorption structures and energetics of molecules on metal surfaces: Bridging experiment and theory," Prog. Surf. Sci. **91**, 72–100 (2016).
[104]P. Milligan, J. McNamarra, B. Murphy, B. C. C. Cowie, D. Lennon, and M. Kadodwala, "A NIXSW and NEXAFS investigation of thiophene on Cu (111)," Surf. Sci. **412**, 166–173 (1998).
[105]G. Liu, J. A. Rodriguez, J. Dvorak, J. Hrbek, and T. Jirsak, "Chemistry of sulfur-containing molecules on Au (111): Thiophene, sulfur dioxide, and methanethiol adsorption," Surf. Sci. **505**, 295–307 (2002).
[106]A. Imanishi, T. Yokoyama, Y. Kitajima, and T. Ohta, "Structural and electronic properties of adsorbed thiophene on Cu (111) studied by S K-edge x-ray absorption spectroscopy," Bull. Chem. Soc. Jpn. **71**, 831–835 (1998).
[107]G. Vidali, G. Ihm, H.-Y. Kim, and M. W. Cole, "Potentials of physical adsorption," Surf. Sci. Rep. **12**, 135–181 (1991).
[108]R. D. Diehl, T. Seyller, M. Caragiu, G. S. Leatherman, N. Ferralis, K. Pussi, P. Kaukasoina, and M. Lindroos, "The adsorption sites of rare gases on metallic surfaces: A review," J. Phys.: Condens. Matter **16**, S2839 (2004).
[109]V. G. Ruiz, W. Liu, and A. Tkatchenko, "Density-functional theory with screened van der Waals interactions applied to atomic and molecular adsorbates on close-packed and non-close-packed surfaces," Phys. Rev. B **93**, 035118 (2016).
[110]P. L. Silvestrelli and A. Ambrosetti, "van der Waals-corrected density functional theory simulation of adsorption processes on noble-metal surfaces: Xe on Ag (111), Au (111), and Cu (111)," J. Low Temp. Phys. **185**, 183–197 (2016).
[111]É. D. Murray, K. Lee, and D. C. Langreth, "Investigation of exchange energy density functional accuracy for interacting molecules," J. Chem. Theory Comput. **5**, 2754–2762 (2009).
[112]J. P. Perdew and W. Yue, "Accurate and simple density functional for the electronic exchange energy: Generalized gradient approximation," Phys. Rev. B **33**, 8800 (1986).
[113]H. Tang, S. T. u. R. Chowdhury, and J. P. Perdew, "Revised SCAN+rVV10" (unpublished) (2021).